Nitrogen Oxides Emissions Estimation for a hydrogen-fuelled Dual-Mode Ramjet in the conceptual design phase

HiSST: 3rd International Conference on
High-Speed Vehicle Science Technology
14 -19 April 2024, Busan, Korea

Nitrogen Oxides Emissions Estimation for a hydrogen-fuelled Dual-Mode Ramjet in the conceptual design phase

Valeria Borio[1], Roberta Fusaro[2], Nicole Viola[3], Guido Saccone[4] and Ginevra Cianci[5]

Abstract

This paper aims to investigate the P_3-T_3 method originally developed for nitrogen oxide emissions estimation of subsonic kerosene-fuelled aircraft and to extend its applicability to an unconventional high-speed propulsive system and hydrogen fuelling. For this purpose, the introduction of two new variables, namely the Mach number and the Damköhler number, proves to extend the applicability of the analytical formulation up to Mach 8. The new formulation is developed thanks to the availability of 1D chemical-kinetic simulations of the combustor of the Dual-Mode Ramjet engine installed onboard the STRATOFLY MR3 vehicle, a hypersonic civil transportation vehicle with a waverider configuration. Moreover, in an effort to verify the independence of the novel P_3-T_3 formulation from the reference emissive database, the DLR-Stöppler formulation was considered. The upgrade of the P_3-T_3 method allows the mean estimation error to be reduced from 17.28%, resulting from the original formulation, to 0.399% of the novel formulation. The updated DLR-Stöppler method provided nitrogen oxide emissions assessments with a mean error of 0.405%, comparable with those of the novel P_3-T_3 method.

Keywords: *high-speed aircraft, hydrogen-fuelling, conceptual design, green aviation*

Nomenclature

ATR – Air-Turbo Rocket
CO_2 – Carbon Dioxide
DMR – Dual-Mode Ramjet
EINO – Nitric Oxide Emissions Index
GHG – Greenhouse Gas
H_2O – Water Vapour
LH2 – Liquid Hydrogen
NO_x – Nitrogen oxides
SAF – Sustainable Aviation Fuels

1. Introduction

The current globalized world raises the demand for faster and more efficient connections among different areas of the Planet and its satisfaction will be essential for the future thriving of our society. This scenario is in contrast with the necessity of minimizing Greenhouse gas (GHG) emissions urged by the global climate crisis faced by the Earth. Currently, aircraft emissions account for 2.1% of all man-made carbon dioxide (CO_2) emissions and 12% of emissions by the transport sector [1], but their impact on climate change will likely worsen in the next decades as air traffic is expected to grow by a factor of more than two by 2050 [2]. As a response, the aerospace sector has focused on studying alternative fuels to conventional Jet-A1, which are represented by Sustainable Aviation Fuels (SAF) and liquid hydrogen (LH_2). SAF are aviation fuels derived from non-fossil sources, both biological and non-biological, having an energy density comparable to conventional jet fuels. They are considered the most ready-to-use alternatives to Jet-A1, also known as "drop-in" fuels, since they can be used in blends

[1] *Politecnico di Torino, Corso Duca degli Abruzzi 24, 10129 Turin, Italy, valeria.borio@polito.it*
[2] *Politecnico di Torino, Corso Duca degli Abruzzi 24, 10129 Turin, Italy, roberta.fusaro@polito.it*
[3] *Politecnico di Torino, Corso Duca degli Abruzzi 24, 10129 Turin, Italy, nicole.viola@polito.it*
[4] *Italian Aerospace Research Centre, Via Maiorise, 81043 Capua, Italy, g.saccone@cira.it*
[5] *Politecnico di Torino, Corso Duca degli Abruzzi 24, 10129 Turin, Italy, s302521@studenti.polito.it*

with kerosene without requiring the adaptation of the aircraft or the ground infrastructure. The combustion of SAF blends allows the reduction of aircraft emissions, in particular CO_2, related to both aircraft operations and fuel production. A further reduction of emissions and noise pollution can be achieved with LH_2 fuelling, provided that hydrogen is produced from a renewable source. However, the use of LH_2 requires a significant redesign of the aircraft's engine and airframe and the ground infrastructure, thus making it a viable solution only for the long term [3]. Although the transition to hydrogen-fuelling will enable the decarbonization of the aviation sector, all the other climate-altering emissions, including nitrogen oxides (NO_x) and water vapor (H_2O), will still need to be monitored and minimized since the conceptual design stage. As a matter of fact, these substances have a harmful influence on climate, especially when emitted in the stratosphere, i.e. at typical flight altitudes of supersonic and hypersonic aircraft, where they have a longer lifetime. Water vapor enhances surface warming both directly through the greenhouse effect and indirectly by influencing the formation of polar stratospheric clouds and ozone (O_3) depletion [4]. The latter is further affected by the presence of NO_x molecules, which act as catalysts in the ozone depletion mechanism, even in small concentrations [5]. Given the expected increase in H_2O and NO_x emissions caused by the entry into service of a high-speed fleet for civil transport operating at higher altitudes and by the transition from fossil fuels to hydrogen, it is fundamental to evaluate the environmental impact since the early stages of the design process [6]. Literature offers a variety of methods for NO_x emission estimation modelling. Among them, simplified physics-based models and high-fidelity simulations provide accurate results, but their application requires the knowledge of complex kinetic mechanisms and the detailed geometry of the combustor, making them usually inapplicable for emissions estimations in the early stages of design. The correlation-based models are usually developed from experimental data of specific engines, thus preventing their extension to all engines. In this category, the P_3-T_3 model is widely used, especially at the industrial level, since it is the most accurate. However, it requires proprietary data, namely pressure and temperature at the inlet of the combustion chamber, which may not yet be available in the conceptual design stage. This issue is solved by the fuel-flow method, albeit with a limited reduction of the prediction accuracy [7].

For the work presented in this paper, the P_3-T_3 method is selected for evaluating NO_x emissions since the authors can benefit from the legacy data of the H2020 STRATOFLY project [8]. However, since the P_3-T_3 method was originally conceived for subsonic kerosene-fuelled turbofan engines, this work aims to investigate the NO_x emissions estimation ability of this model for subsonic kerosene-fuelled aircraft and to extend its capability to an unconventional high-speed propulsive system, namely the DMR, and hydrogen fuelling. Within the H2020 STRATOFLY project, an analogous work has been successfully carried out for the Air-Turbo Rocket engine [9]. However, the implementation of the P_3-T_3 method in the DMR engine faces some additional challenges. Indeed, differently from the ATR engine, the sea level conditions cannot be selected as reference data for the P_3-T_3 method, since the DMR is not able to work at ground level. Moreover, due to the nature of supersonic combustion, some additional physical phenomena such as the interaction of shock waves along the engine duct must be taken into account. As a consequence, a 1D modelling of the combustion process occurring in the DMR engine is required for the case study, since the 0D chemical kinetic simulations employed for the ATR would represent an extremely simplified representation of supersonic combustion [9].

2. Case study

Funded by the European Commission within the EU Horizon 2020 framework program, the STRATOFLY project aims to assess the technical and operational feasibility of high-speed civil stratospheric flights. A major achievement of the project was the design of the STRATOFLY MR3 vehicle concept, which is a waverider powered by six ATR engines and a single DMR. The ATR engines are operated from take-off up to Mach 4, after which they are gradually shut down while the DMR is activated to reach Mach 8. The cruise takes place at Mach 8 between 32 and 36 km of altitude. Once a proper distance from the landing site has been reached, the aircraft begins a propelled descent. Considering this mission profile, the STRATOFLY MR3 vehicle can fly from Brussels to Sidney in 3 hr and 24 min [10]. All engines are connected to form a Turbine Based Combined Cycle (TBCC) and they are fuelled with liquid hydrogen. Regarding the internal flow path, the air entering the inlet is split into two ducts: the upper one goes to the DMR engine while the side one feeds the ATR engines. The air flowing in the ATR duct passes through a compressor before the combustion chamber whereas in the DMR channel, the compression occurs on the inlet ramps and isolator. The combustion products are then discharged through a common

nozzle [11, 12]. The layout of the highly integrated propulsive system is shown in Fig 1. Due to the complexity of the propulsive architecture of the STRATOFLY MR3 vehicle, the present work is focused on the DMR engine.

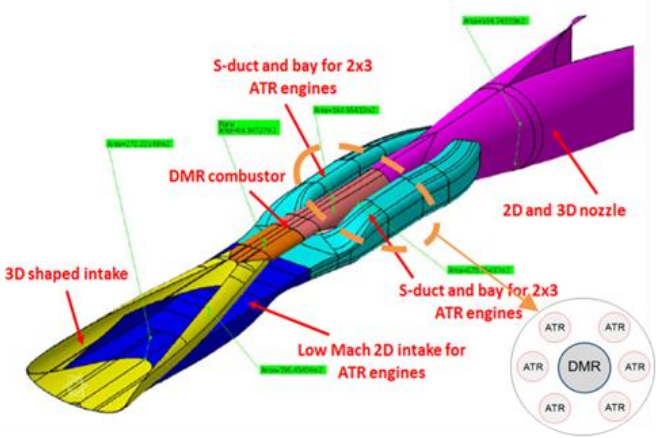

Fig 1. External view of the flowpaths in the engine duct [8].

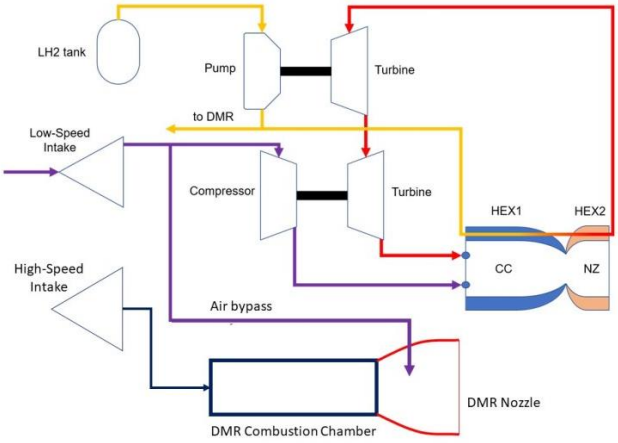

Fig 2. Schematic representation of the combined cycle [10].

2.1. Propulsive and emissive database

A propulsive and emissive database, for both the ATR and the DMR, was developed during the project with the CIRA in-house SPREAD code and is here used as an important set of input data [12]. The propulsive model of the combined cycle shown in Fig 2 has been developed with the EcoSimPro software, which is a multidisciplinary simulation tool capable of replicating the physical behaviour of various engine components. This model has been used to evaluate the thermodynamic and propulsive performance of the ATR and DMR engines for a set of flight and reference points for the mission considered. This step is instrumental for the calculation of NO_x emission indexes (EINO), as the thermodynamic data resulting from the propulsive modelling is fed as input to the emission estimation tool, corresponding here to the SPREAD code. The emissive database for the ATR has been obtained with 0D chemical kinetic simulations while for the DMR 1D computations have been performed, in order to include other relevant physical phenomena, such as the interaction of shock waves along the propulsive power system. These simulations have been performed considering the Z22_NO_x20 kinetic mechanism which results from the combination of the Z22 kinetic mechanism, developed by Zetterval and Fureby specifically for hydrogen/oxygen combustion, with the twenty reactions for NO_x formation [13, 14]. The Z22 kinetic mechanism has been selected for the case study after a 0D kinetic assessment, carried out with Cantera, to provide accurate predictions of ignition delay times and NO_x emissions with respect to the other available mechanisms [15]. Furthermore, NO_x formation has been taken into account by including a detailed H/O/N sub-mechanism including not only the Zeldovich reactions [16], which corresponds to the prevalent NO_x formation mechanism in the DMR due to the high temperatures reached inside the engine, but also further chemical pathways involving NH_3, N_2H, and HNO which have been proved to play an important role in the production of NOx, especially in fuel-rich conditions.

2.2. The DMR engine

A DMR engine is an advanced propulsive system able to function both as a ramjet and as a scramjet. As shown in Fig 3, a typical scramjet is composed of a supersonic-hypersonic intake, an isolator, a combustor and a nozzle. The absence of turbomachinery is one of the aspects that makes it an interesting solution for high-speed propulsion since it significantly decreases the risk of mechanical failures. The airflow entering the engine is dynamically compressed by the intake through the interaction between oblique shock waves and the boundary layer. The flow then passes through the isolator, whose function is to separate the intake from the combustor and to prevent the flow return back due to the pressure rise in the combustion chamber. Here, the flow is mixed with the fuel, and it is combusted in supersonic conditions. Finally, the exhaust gases are discharged through a divergent nozzle which accelerates them as close as possible to the flight speed. This type of engine requires the intake and the nozzle to be very long and integrated into the airframe, due to the very low shock wave angle generated at the nose and the large expansion ratio at the exhaust outlet. The most significant challenge faced in the study of the DMR engine is represented by the high complexity of the fluid dynamics of the supersonic and hypersonic flow, due to the various phenomena such as the presence of shock and expansion waves in the engine duct, the different fuel-air mixing mechanism involved, and supersonic combustion. Additional issues are presented in the chemical processes involved, since at high Mach numbers the airflow temperature significantly rises, and the dissociation process is activated. Moreover, a hotter incoming airflow causes an increase in the combustion temperature, with the risk of negatively affecting the materials. All issues mentioned should be accurately considered during the design of a scramjet engine [11].

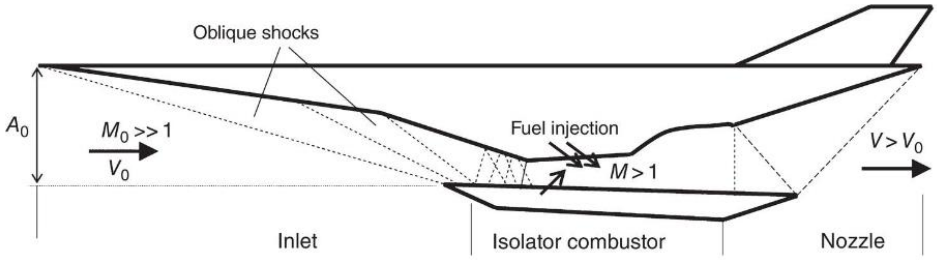

Fig 3. Schematic representation of a scramjet engine operating in dual-mode [11].

3. Methodology

The methodology followed to adapt the P_3-T_3 method to the DMR engine is presented in Fig 4.

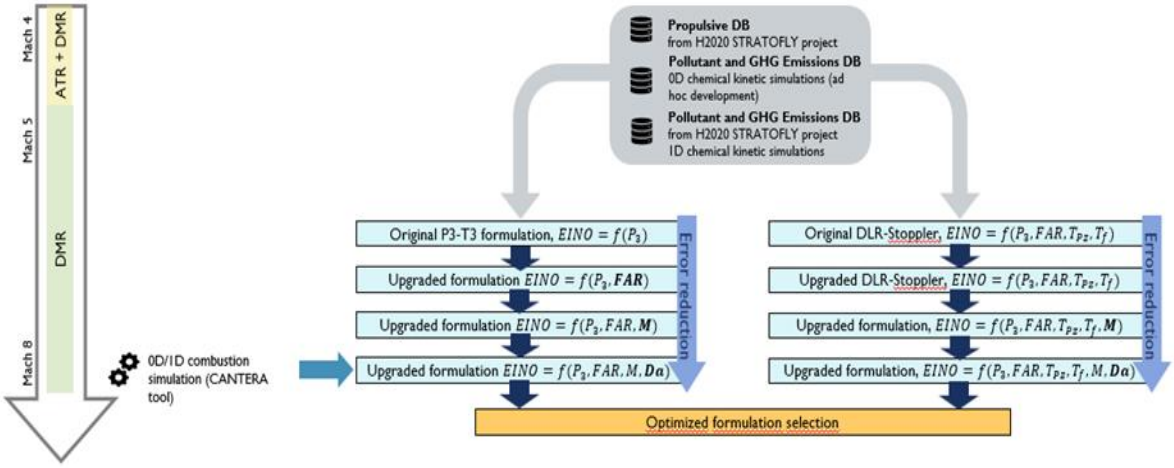

Fig 4. Methodology implemented for the adaptation of the P_3-T_3 method to the case study.

In an effort to verify the independence of the methodology from the database, the DLR-Stöppler method was considered [17]. Since this formulation was also originally tailored for subsonic kerosene-

fuelled turbofans, it has been updated to the case study according to the same methodology followed for the P_3-T_3 method.

3.1. Reference conditions

The implementation of both the P_3-T_3 method and the DLR-Stöppler one requires the knowledge of a set of reference conditions, which represents a major challenge for the case study. As a matter of fact, since the DMR cannot work at ground level, a new suitable reference condition had to be selected for this engine. Therefore, with the aim of recreating the throttle setting suggested by the ICAO Annex 16 [18], the Mach 6 condition has been identified as the 100% value of thrust from which the additional four throttle settings have been deduced, as shown in Fig 5. It is worth noting that the throttle levels considered in this work are slightly different than those indicated by the ICAO in order to better adapt them to DMR operations.

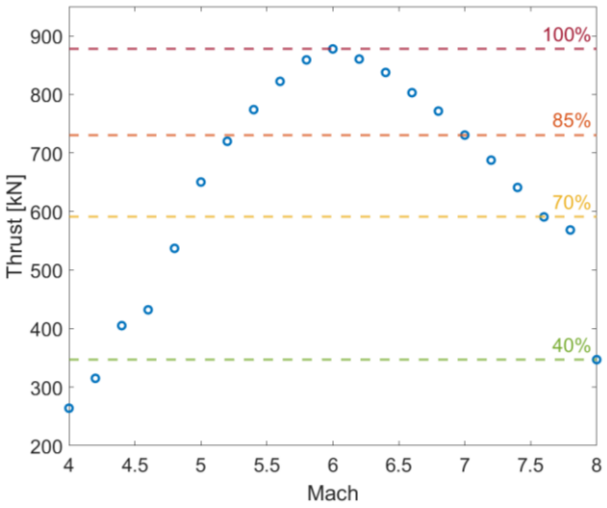

Fig 5. DMR thrust profile and throttle settings selected as reference conditions.

Even though it is shown in Fig 5, the mission profile's segment between Mach 4 and 5 has been excluded from this analysis as it represents the transition phase from pure ATR to solely DMR operations. Consequently, the propulsive and emissive databases show a high level of uncertainty in the data within this interval.

3.2. Methodology overview

As shown in Fig 4, the initial step of methodology consists of applying the original P_3-T_3 formulation:

$$EINO_{FL} = EINO_{REF} \cdot \left(\frac{P_{3,FL}}{P_{3,SL}}\right)^{n} \cdot \left(\frac{FAR_{FL}}{FAR_{SL}}\right)^{m} \cdot e^{H} \quad (1)$$

with $n = 0.4$ and $m = 0$. In Eq. (1), the NO_x emissions are calculated as a function of the sole combustor inlet pressure p_3, since the term containing the fuel-to-air ratio (FAR) is counted as a unitary factor. The term H is a humidity correction which is dependent on the atmospheric conditions at flight altitude [7]. The NO_x emissions indices at reference conditions ($EINO_{SL}$) contained in the STRATOFLY emissive database are generally obtained as the ratio between the mass fractions of NO_x generated by the combustion and the LH_2 burned. The first attempt at upgrading the P_3-T_3 method to hydrogen-fuelled high-speed propulsion is the optimization of the exponents *n* and *m*, in an effort to also factor in the effect of the fuel-to-air ratio, which in ATR and DMR engines has a greater influence than in conventional turbofans powered by kerosene. As a matter of fact, independently from the choice of fuel, the fuel-to-air ratio directly influences the adiabatic flame temperature (T_{FL}) reached in the combustor chamber, which in turn impacts NO_x formation. In particular, T_{FL} reaches a peak around the stoichiometric composition of the fuel/air mixture, leading to maximum NO_x emissions at this point. Therefore, a lean mixture is usually preferred for the minimization of NO_x, allowing in the case of LH_2 fuelling to also avoid additional complex reaction pathways which will be more difficult to evaluate [9].

Given the different mission types of high-speed vehicles with respect to traditional aircraft, the impact of the variation of flight level conditions on NOx emissions was considered in the following step by

including the Mach number. As a matter of fact, this parameter is not only a direct indicator of the flight speed, but it also varies as a function of the atmospheric pressure and temperature at different altitudes. The formulation resulting from this step of the flowchart is:

$$\mathrm{EINO}_{FL} = \mathrm{a} \cdot EINO_{SL} \cdot \left(\frac{P_{3,FL}}{P_{3,SL}}\right)^{n} \cdot \left(\frac{FAR_{FL}}{FAR_{SL}}\right)^{m} \cdot e^{H} \cdot M^{d} \tag{2}$$

In the final upgraded P_3-T_3 formulation, the combustion efficiency is considered by means of including the Damköhler number, obtained as

$$Da = \frac{\tau_{res}}{\tau_{ign}} \tag{3}$$

where τ_{res} is the residence time of the hydrogen/air mixture in the combustion chamber and τ_{ign} is its ignition delay time, both computed by the Cantera software. The introduction of this parameter is strictly related to NO_x minimization strategies for advanced high-speed propulsive systems. As a matter of fact, the residence time is generally higher than the ignition delay time, so $Da > 1$. However, in the DMR engine, the residence time should be sufficient for the completion of the combustion process but not too high as to increase the NO_x emissions. The final upgraded P_3-T_3 formulation is:

$$EINO_{FL} = a \cdot EINO_{SL} \cdot \left(\frac{P_{3,FL}}{P_{3,SL}}\right)^{n} \cdot \left(\frac{FAR_{FL}}{FAR_{SL}}\right)^{m} \cdot e^{H} \cdot M^{d} \cdot \left(\frac{Da_{FL}}{Da_{SL}}\right)^{b} \tag{4}$$

The exponents of every subsequent formulation are optimized at each step with a nonlinear optimization conducted in Matlab.

3.3. Input data

Concerning the input data, the values of pressure, fuel-to-air ratio, and EINO considered are those issued in the STRATOFLY databases. On the contrary, the data related to the chemical kinetics of the combustion process, including the ignition delay, the residence times, and the adiabatic flame temperatures, have been calculated with the 0D/1D Cantera software simulations [19] using the Z22_NO_x20 kinetic mechanism [14]. These results have been interpolated with polynomial laws from which the input data for the P_3-T_3 method and the DLR-Stöppler method have been determined.

4. Results and discussion

The methodology presented in Fig 4 leads to the definition of four independent and optimized formulations, whose exponents are reported in Table 1.

Table 1. Exponents of the upgraded formulations of the P_3-T_3 method.

Formulation	a	n	m	d	b
Original EINO=f(p_3)	1	0.4	0	-	-
EINO=f(p_3,FAR)	1	-3.31	10.54	-	-
EINO=f(p_3,FAR,M)	1	10.34	11.91	-0.31	-
EINO=f(p_3,FAR,M,Da)	1	26.34	9.10	-0.61	0.12

As expected, the errors related to the NO_x emissions estimation decrease with every additional variable included in the formulation, showing promising results in terms of estimation accuracy, as can be observed in Fig 6 and in Fig 7.

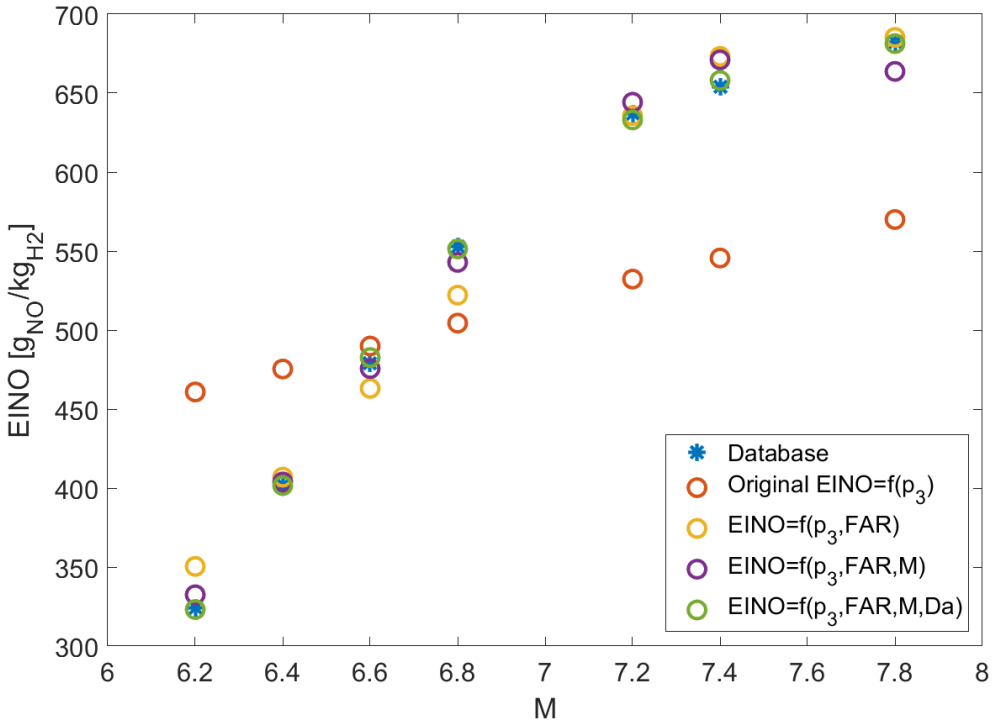

Fig 6. EINO estimation for the DMR.

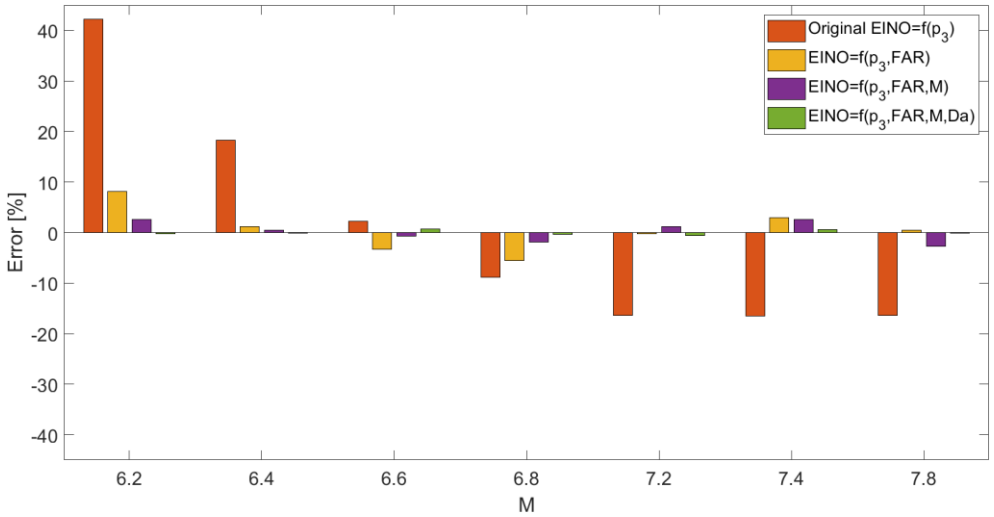

Fig 7. EINO estimation errors for the DMR.

The mean errors for each formulation are reported in Table 2.

Table 2. Mean errors for the upgraded formulations of the P_3-T_3 method.

Formulation	Mean errors
Original EINO=f(p_3)	17.28 %
EINO=f(p_3,FAR)	3.13 %
EINO=f(p_3,FAR,M)	1.72 %
EINO=f(p_3,FAR,M,Da)	0.40 %

The most accurate NO_x emissions estimation is obtained with the P_3-T_3 formulation shown in Eq. (5),

$$EINO_{FL} = EINO_{SL} \cdot \left(\frac{P_{3,FL}}{P_{3,SL}}\right)^{26.34} \cdot \left(\frac{FAR_{FL}}{FAR_{SL}}\right)^{9.10} \cdot e^{H} \cdot M^{-0.61} \cdot \left(\frac{Da_{FL}}{Da_{SL}}\right)^{0.12} \quad (5)$$

which results in a mean error of 0.40%. The optimized exponents of the upgraded P_3-T_3 formulation of Eq. (5) are consistent with the chemical and physical behaviour expected for each input variable:

- since in the DMR the combustor inlet pressure at flight level is of the same order of magnitude as that at the reference conditions, which in turn do not coincide with the actual sea level, the p_3 ratio has an approximately unit value for the mission segment considered. However, p_3 still gives a positive contribution to NO_x formation, i.e. an increasing pressure value leads to higher NO_x emissions. However, in order to count the effect of p_3 on EINO levels in the DMR equally to the ATR [9], the exponent *m* reaches a higher value;
- concerning the FAR, the rise of its value (still below the stoichiometric point) leads to an increase in NO_x emissions. Analogously to the p_3, the ratio between its value at flight level and reference conditions is almost unitary, thus its effect on EINO estimation has to be factored in by a large value of the exponent *n*;
- the Mach number is counted in the measure of a square root denominator, meaning that it has a negative effect on NO_x formation. Despite the apparent contradiction with the expected behaviour, the reason behind this result lies in the capability of the Mach number to capture the flight level variation. As a matter of fact, at the flight altitudes related to DMR operations, the decrease in static atmospheric pressure (p_0) cannot be compensated by the increase in Mach number in their contribution to total dynamic pressure, leading to an overall reduction of the combustion inlet temperature over Mach;
- the Damköhler number ratio shows a proportional correlation with EINO levels, meaning that a higher value of this term results in an increment of NO_x emissions. Since the ignition time is computed based on the chemical kinetic of the hydrogen/air mixture, the increase in Da is caused by the extension of the residence time, which in turn raises the temperature of the gases in the combustion chamber, resulting in more prolific NO_x formation. Therefore, it is of utmost importance to accurately match these two characteristic times.

As can be seen in Fig 6 and Fig 7, a significant improvement of the prediction capability of the P_3-T_3 method for high-speed hydrogen-fuelled transportation systems can already be appreciated from the inclusion of FAR, while the addition of M and Da allows to obtain an almost exact EINO estimation. Therefore, each formulation can be considered independent, and it can be employed depending on the availability of the input variables at various stages of the conceptual design phase.

The update of the DLR-Stöppler method has been carried out following the same methodology used for the P_3-T_3 method. The original formulation of DLR-Stöppler method is:

$$EINO_x = EINO_{x,REF} \cdot \left(\frac{1+\frac{1}{FAR}}{1+\frac{1}{FAR_{Ref}}}\right)^{\beta} \cdot \frac{\dot{m}_{air,REF}}{\dot{m}_{air}} \cdot \left(\frac{p_3}{p_{3,REF}} \cdot \frac{T_{PZ,REF}}{T_{PZ}}\right)^{c} \cdot e^{\frac{E}{R}\left(\frac{1}{T_{FL}} - \frac{1}{T_{FL,REF}}\right)} \quad (6)$$

where $\dot{m}_{air}$ is air mass flow rate, T_{PZ} is the primary zone temperature, T_{FL} is the adiabatic flame temperature, E is the activation energy of the slowest Zeldovich reaction, R is the universal gas constant. The values of T_{PZ} and T_{FL} are dependent on the temperature reached in thermodynamic equilibrium conditions, which can be computed with the aid of the Cantera software, and on the homogeneity of the hydrogen/air mixing [17].

Analogously to the P_3-T_3 method, four different formulations have been derived, whose exponents have been optimized at each following step. The resulting exponents are shown in Table 3.

Table 3. Exponents of the upgraded formulations of the DLR-Stöppler method.

Formulation	a	β	c	d	b
Original EINO=f(p_3,FAR,T_{PZ}, T_{FL})	1	-0.55	1.37	-	-
EINO=f(p_3,FAR,T_{PZ}, T_{FL})	1	-8.99	-0.43	-	-

EINO=f(p_3,FAR,T_{PZ}, T_{FL},M)	1	-18.54	22.53	-0.47	-
EINO=f(p_3,FAR,T_{PZ}, T_{FL},M,Da)	1	-18.54	22.79	-0.47	-0.01

The EINO estimated with upgraded formulations of the DLR-Stöppler method, and the related errors are shown in Fig 8 and Fig 9.

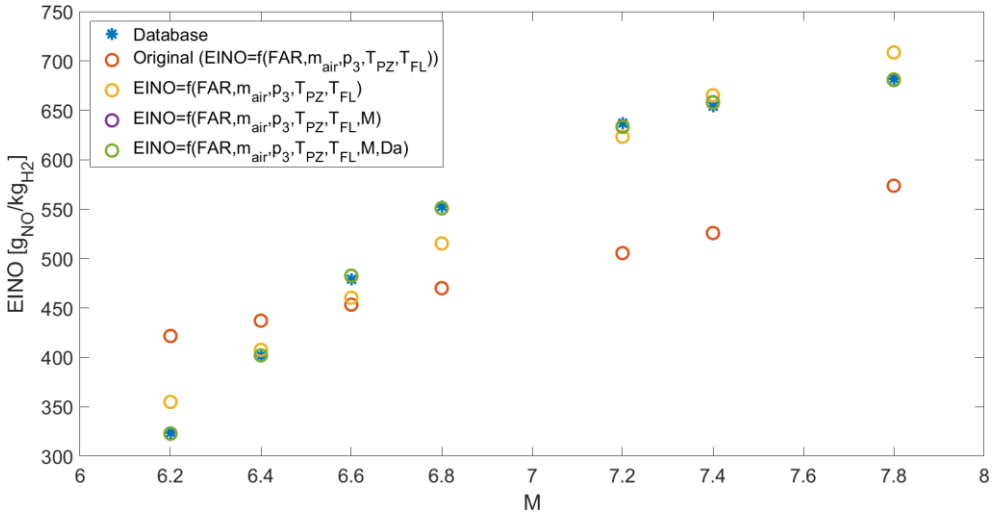

Fig 8. EINO estimation for the DMR with the upgraded DLR-Stöppler method.

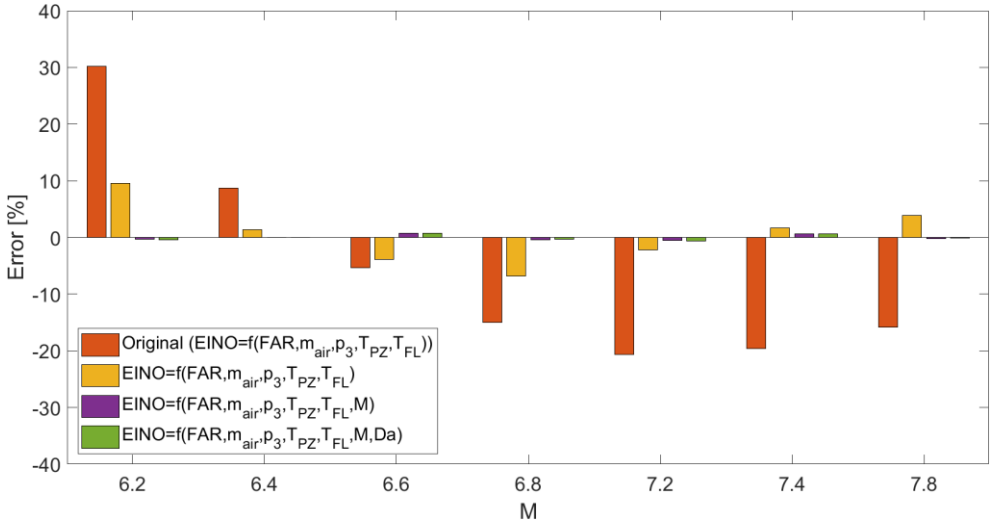

Fig 9. EINO estimation errors for the DMR with the upgraded DLR-Stöppler method.

The mean errors of each formulation obtained following the upgrade methodology for the DLR-Stöppler are listed in Table 4.

Table 4. Mean errors for the upgraded DLR-Stöppler method.

Formulation	Mean errors
Original EINO=f(p_3,FAR,T_{PZ}, T_{FL})	16.48 %
EINO=f(p_3,FAR,T_{PZ}, T_{FL})	4.20 %
EINO=f(p_3,FAR,T_{PZ}, T_{FL},M)	0.404 %
EINO=f(p_3,FAR,T_{PZ}, T_{FL},M,Da)	0.402 %

Similarly, to the P_3-T_3 method, the application of the upgraded formulations DLR-Stöppler method leads to increasingly accurate NO_x assessments, with the minimum mean estimation error equal to 0.402%, obtained with the formulation derived in the final step of the flowchart, which is:

$$EINO_x = EINO_{x,REF} \cdot \left(\frac{1+\frac{1}{FAR}}{1+\frac{1}{FAR_{Ref}}} \right)^{-18.54} \cdot \frac{\dot{m}_{air,REF}}{\dot{m}_{air}} \cdot \left(\frac{p_3}{p_{3,REF}} \cdot \frac{T_{PZ,REF}}{T_{PZ}} \right)^{22.79} \cdot e^{\frac{E}{R}\left(\frac{1}{T_{FL}} - \frac{1}{T_{FL,REF}}\right)} \cdot M^{-0.47} \cdot \left(\frac{Da}{Da_{REF}} \right)^{-0.01} \quad (7)$$

The EINO estimated with Eq. (**5**) and Eq. (**7**) are shown in Fig 10 and Fig 11. As can be observed the estimation accuracy of the upgraded DLR-Stöppler method is similar to that of the P_3-T_3 method. However, the latter is usually preferred in the conceptual design stage since it requires fewer and more accessible input parameters, whereas the DLR-Stöppler method includes variables related to the chemical kinetic simulation of the combustion, which are generally more difficult to obtain in the early stages of the design process.

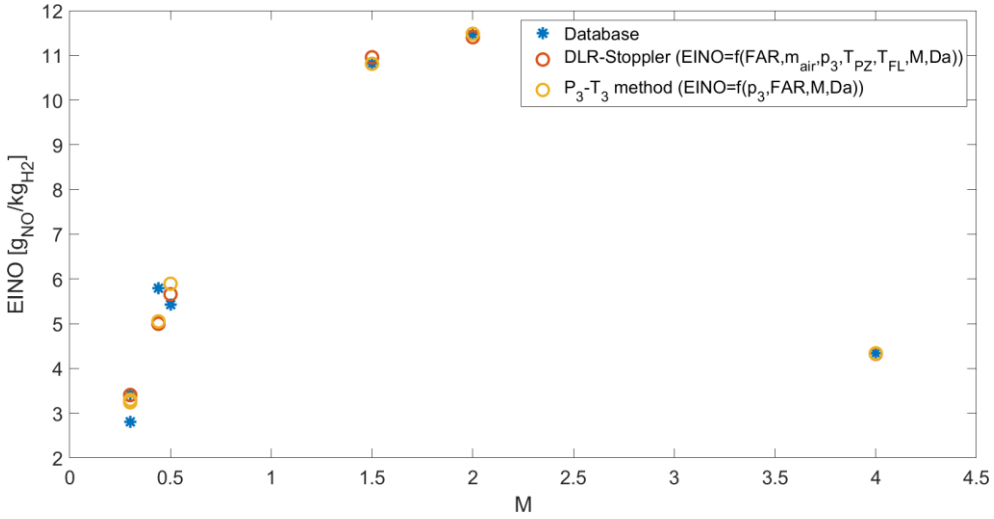

Fig 10. Comparison of EINO estimated with the upgraded formulations of the P3-T3 method and DLR-Stöppler method.

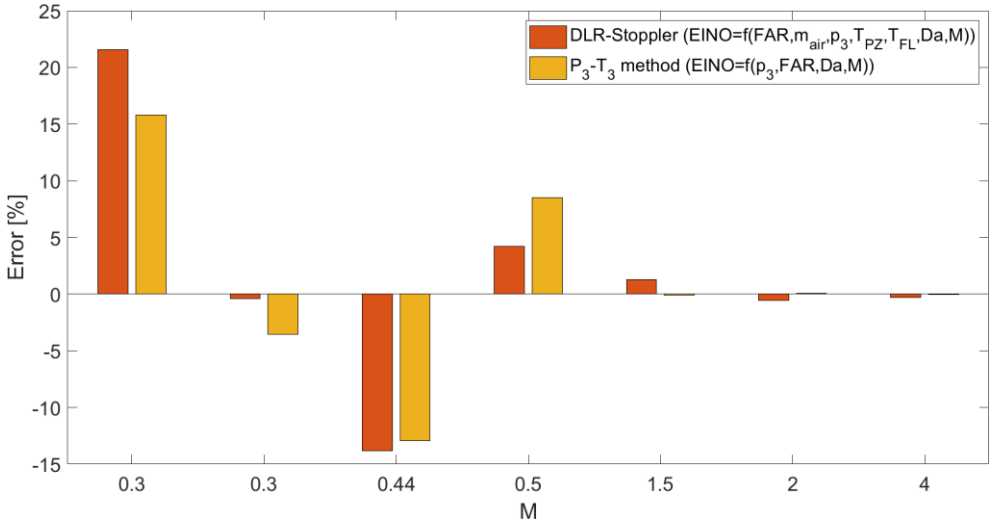

Fig 11. Comparison of EINO estimation errors with the upgraded formulations of the P3-T3 method and DLR-Stöppler method.

References

1. Air Transport Action Group (ATAG).: Facts and Figures. https://www.atag.org/facts-figures/. Accessed 27 October 2023
2. ICAO: ICAO Environmental Report 2022 (2022)

3. Bauen, A., Bitossi, N., German, L., Harris, A., Leow, K.: Sustainable Aviation Fuels. In: Johnson Matthey Technology Review 64, 263–278, (2020). https://doi.org/10.1595/205651320X15816756012040
4. Schumann, U.: Aircraft Emissions. In: Encyclopedia of Global Environmental Change, Vol. 3, pp. 178-186. John Wiley & Sons, Ltd, Chichester (2002)
5. Ingenito, A.: Impact of hydrogen fueled hypersonic airliners on the O_3 layer depletion. International Journal of Hydrogen Energy 43, pp. 22694-22704 (2018). https://doi.org/10.1016/j.ijhydene.2018.09.208
6. Tait, K.N., Khan, M.A.H., Bullock, S., Lowenberg, M.H., Shallcross, D.E.: Aircraft emissions, Their Plume-Scale Effects, and the Spatio-Temporal Sensitivity of the Atmospheric Response: A Review. Aerospace 9, (2022). https://doi.org/10.3390/aerospace9070355
7. Chandrasekaran, N., Guha, A.: Study of Prediction Methods for NOx Emission from Turbofan Engines. Journal of Propulsion and Power 28, pp. 170-180 (2012)
8. Marini, M.: STRATOFLY Periodic Technical Report - Report II (2021)
9. Viola, N., Fusaro, R., Saccone, G.; Borio, V.: Analytical Formulations for Nitrogen Oxides Emissions Estimation of an Air Turbo-Rocket Engine Using Hydrogen. Aerospace 10, 909 (2023). https://doi.org/10.3390/aerospace10110909
10. Viola, N., Fusaro, R., Saracoglu, B., Schram, C., Grewe, V., Martinez, J., Marini, M., Hernandez, S., Lammers, K., Vincent, A., Hauglustaine, D., Liebhardt, B., Linke, F., Fureby, C.: Main Challenges and Goals of the H2020 STRATOFLY Project. Aerotecnica, Missili & Spazio 100, pp. 95-110 (2021). https://doi.org/10.1007/s42496-021-00082-6
11. Musielak, D.: Scramjet Propulsion: A Practical Introduction. John Wiley & Sons, Ltd (2022)
12. Saccone, G., Ispir, A.C., Saracoglu, B.H., Cutrone, L., Marini, M.: Computational evaluations of emissions indexes released by STRATOFLY air-breathing combined propulsive system. Aircraft Engineering and Aerospace Technology (2022). ISSN 0002-2667
13. Vincent-Randonnier, A., Sabelnikov, V., Ristori, A., Zettervall, N., Fureby, C.: An experimental and computational study of hydrogen–air combustion in the LAPCAT II supersonic combustor. Proceedings of the Combustion Institute, 37, pp. 3703-3711 (2019). https://doi.org/10.1016/j.proci.2018.05.127
14. Zettervall, N.: Modelling of a reduced NOx reaction sub-mechanism. Preliminary Report, STRATOFLY Project. Swedish Defense Research Agency (2020)
15. Saccone, G., Natale, P., Cutrone, L., Marini, M.: Kinetic Analysis and CFD Modelling of Hydrogen-Air Combustion Applied to Scramjet Vehicles. Proceedings of the 7th World Congress on Momentum, Heat and Mass Transfer (2022)
16. Warnatz, J., Maas, U., Dibble, R.: Combustion: Physical and Chemical Fundamentals, Modeling and Simulation, Experiments, Pollutant Formation. Springer (2006)
17. Silberhorn, D., Dahlmann, K., Görtz, A., Linke, F., Zanger, J., Rauch, B., Methling, T., Janzer, C., Hartmann, J. Climate impact reduction potentials of synthetic kerosene and green hydrogen powered mid-range aircraft concepts. Applied Sciences 12 (2022). http://doi.org/10.3390/app12125950
18. ICAO. Annex 16 Volume II Aircraft Engine Emissions. ICAO, Montreal, QC, Canada, (2014)
19. Goodwin, D.G., Moffat, H.K., Schoegl, I., Speth, R.L., Weber, B.W.: Cantera: An object-oriented software toolkit for chemical kinetics, thermodynamics, and transport processes. (Version 2.6.0). Zenodo (2022). https://doi.org/10.5281/zenodo.6387882